Millimeter and Radio Observations of z∼6 Quasars

Ran Wang

Astronomy Department, Peking University, Beijing 100871, China

National Radio Astronomy Observatory, PO Box 0, Socorro, NM, USA 87801

rwang@nrao.edu

Chris L. Carilli

National Radio Astronomy Observatory, PO Box 0, Socorro, NM, USA 87801

ccarilli@aoc.nrao.edu

Alexandre Beelen

Argelander-Institut für Astronomie, University of Bonn, Auf dem Hügel 71, 53121 Bonn, Germany

Institut d'Astrophysique Spatiale, Université de Paris-Sud, F-91405 Orsay, France

abeelen@astro.uni-bonn.de

Frank Bertoldi

Argelander-Institut für Astronomie, University of Bonn, Auf dem Hügel 71, 53121 Bonn, Germany

bertoldi@astro.uni-bonn.de

Xiaohui Fan

Steward Observatory, The University of Arizona, Tucson, AZ 85721

fan@as.arizona.edu

Fabian Walter

Max-Planck-Institute for Astronomy, Königsstuhl 17, 69117 Heidelberg, Germany

walter@mpia.de

Karl M. Menten

Max-Plank-Institute for Radioastronomie, Auf dem Hügel 71, 53121 Bonn, Germany

kmenten@mpifr-bonn.mpg.de

Alain Omont

Institut d'Astrophysique de Paris, CNRS and Universite Pierre et Marie Curie, Paris, France

omont@iap.fr

Pierre Cox

Institute de Radioastronomie Millimetrique, St. Martin d'Heres, F-38406, France

cox@iram.fr

Michael A. Strauss

Department of Astrophysical Sciences, Princeton University, Princeton, NJ, USA, 08544

strauss@astro.princeton.edu

Linhua Jiang

Steward Observatory, The University of Arizona, Tucson, AZ 85721

jiang@as.arizona.edu

ABSTRACT

We present millimeter and radio observations of 13 SDSS quasars at reshifts z∼6. We observed eleven of them with the Max-Planck Millimeter Bolometer Array (MAMBO-2) at the IRAM 30m-telescope at 250 GHz and all of them with the Very Large Array (VLA) at 1.4 GHz. Four sources are detected by MAMBO-2 and six are detected by the VLA at $\gtrsim 3\sigma$ level. These sources, together with another 6 published in previous papers, yield a submillimeter/millimeter and radio observed SDSS quasar sample at z∼6. We use this sample to investigate the far-infrared (FIR) and radio properties of optically bright quasars in the early universe. We compare this sample to lower redshift samples of quasars observed in the submillimeter and millimeter wavelengths ((sub)mm), and find that the distribution of the FIR to B band optical luminosity ratio (L_{FIR}/L_B) is similar

from z∼2 to 6. We find a weak correlation between the FIR luminosity (L_{FIR}) and B band optical luminosity (L_B) by including the (sub)mm observed samples at all redshifts. Some strong (sub)mm detections in the z∼6 sample have radio-to-FIR ratios within the range defined by star forming galaxies, which suggests possible co-eval star forming activity with the powerful AGN in these sources. We calculate the rest frame radio to optical ratios ($R^*_{1.4} = L_{\nu,1.4GHz}/L_{\nu\ 4400\mathring{A}}$) for all of the VLA observed sources in the z∼6 quasar sample. Only one radio detection in this sample, J083643.85+005453.3, has $R^*_{1.4} \sim 40$ and can be considered radio loud. There are no strong radio sources ($R^*_{1.4} \geq 100$) among these SDSS quasars at z∼6. These data are consistent with, although do not set strong constraints on, a decreasing radio-loud quasar fraction with increasing redshift.

Subject headings: galaxies: quasars — infrared: galaxies — radio continuum: galaxies — galaxies: starburst — galaxies: high-redshift

1. Introduction

The tight correlation between the mass of supermassive black holes (SMBH) in the centers of galaxies and the bulge mass/velocity dispersion is well documented in the local universe (Magorrian et al. 1998; Marconi & Hunt 2003; Ferrarese & Merritt 2000; Gebhardt et al. 2000; Tremaine et al. 2002) and suggests that the evolution of SMBH and spheroidal galaxies is coupled even at high redshift. Due to the negative K-correction, submillimeter and millimeter ((sub)mm) observations become an efficient way to study the host galaxies of high redshift quasars (Blain & Longair 1993). Such observations probe the rest frame FIR emission from the dust components in the interstellar medium (ISM) of these objects, and thus provide a unique chance to test co-eval black hole and bulge formation by searching for massive starbursts in the host galaxies of high redshift optically bright quasars.

The (sub)mm and radio properties of some optically bright quasars at high redshift are discussed in a number of papers. Observations of large samples of optically selected quasars from z∼1.5 to 5 (Omont 2001, 2003; Carilli et al. 2001; Isaak et al. 2002; Priddey et al. 2003a; Beelen et al. 2004) result in a (sub)mm detection rate of about 30% at mJy sensitivity. The derived far-infrared (FIR) luminosities of the (sub)mm detections are typically $\sim 10^{13}\,L_\odot$ and imply dust masses $\geq 10^8\,M_\odot$. Comparing samples observed with the Max-Planck Millimeter Bolometer (MAMBO) at the 30-meter IRAM telescope at redshift 2 and 4, Omont et al. (2003) found that the FIR luminosities of the optically bright quasars in these samples do not evolve with redshift. Statistical tests for these (sub)mm observed quasars show a weak correlation between the optical and FIR luminosities (Omont et al.

2003; Beelen 2004; Cox et al. 2005), which is argued as an evidence for FIR emission from warm dust heated by star formation. The inferred star formation rate is $\sim 10^3\,M_\odot$ yr^{-1} when assuming a normal initial mass function (IMF). This interpretation is supported by the fact that the radio-to-FIR ratios for the FIR-luminous sources are consistent with the range spanned by star forming galaxies (Carilli et al. 2001; Petric et al. 2006).

The Sloan Digital Sky Survey (SDSS, York et al. 2000) has identified 19 bright quasars at z∼6 (Fan et al. 2000, 2001, 2003, 2004, 2006a). These quasars are unique, in that they are undergoing rapid accretion onto SMBHs with masses $\gtrsim 10^9\,M_\odot$, within 1 Gyr of the Big Bang, an epoch approaching cosmic reionization (Fan et al. 2006c). These z∼6 quasars have been observed at all wavelengths from the X-ray to the radio (eg. Bechtold et al. 2003; Pentericci et al. 2003; Shemmer et al. 2006; Jiang et al. 2006a; Petric et al. 2003). The X-ray to near-infrared (NIR) observations imply Spectral Energy distributions (SEDs) similar to those of local quasars. The integrated bolometric luminosities exceed $\gtrsim 10^{13}\,L_\odot$, and the black hole masses are $\gtrsim 10^9\,M_\odot$ (Willott et al. 2003; Iwamuro et al. 2004; Jiang et al. 2006a). Seven z∼6 SDSS quasars (Fan et al. 2000, 2001, 2003) were observed at 350 GHz with the SCUBA camera at the James Clerk Maxwell Telescope or at 250 GHz with MAMBO. Three are detected by SCUBA (Priddey et al. 2003b; Robson et al. 2004) and two are detected by MAMBO (Bertoldi et al. 2003a). Deep VLA observations at 1.4 GHz were made for six sources, resulting in detections of two of them (Petric et al. 2003; Carilli et al. 2004).

SDSS J114816.64+525150.3 at $z = 6.42$ is the best studied FIR luminous source at z∼6. It was detected with SHARC II, the bolometer camera at the Caltech Submillimeter Observatory at 350 μm, SCUBA at 450 μm and 850 μm, MAMBO at 1.2 mm, and the VLA at 1.4GHz (Beelen et al. 2006; Robson et al. 2004; Bertoldi et al. 2003a; Carilli et al. 2004). Fits to the SED from the FIR to radio imply a warm dust component with a temperature of 55K (Beelen et al. 2006). The corresponding FIR luminosity is $2.2 \times 10^{13}\,L_\odot$ with an inferred dust mass of $4.5 \times 10^8\,M_\odot$. It is also the only z∼6 source that has been detected in the CO and [C II] 158 μm emission lines (Bertoldi et al. 2003b; Walter et al. 2003; Walter et al. 2004; Maiolino et al. 2005). These CO observations reveal a large mass of molecular gas ($\sim 2 \times 10^{10}\,M_\odot$) in the host galaxy.

The (sub)mm through radio observations of J114816.64+525150.3 argue for a massive starburst in its host galaxy, because (i) the FIR to radio ratio of this source follows that of typical star forming galaxies in the local universe (Yun et al. 2001; Carilli et al. 2004), (ii) the huge amount of molecular gas in its host galaxy can provide the required fuel for massive star formation, and (iii) the star formation rates indicated by both FIR luminosity and [C II] 158μm line luminosity are $\sim 10^3$ $M_\odot$ yr^{-1} (Bertoldi et al. 2003a; Maiolino et al. 2005).

Nineteen z∼6 SDSS quasars have been published to date (Fan et al. 2006b). These are an optically selected sample at the highest redshift. We are pursuing a series of (sub)mm through radio studies on this sample in order to (i) find the general dust and gas properties in the host galaxies of these highest redshift quasars, and (ii) search for star formation activity co-eval with the rapid growth of SMBHs in the early universe.

In this paper, we present new MAMBO-2 250 GHz observations of eleven, and VLA 1.4GHz observations of thirteen, z∼6 SDSS quasars. Then, together with previously published results, we discuss the general far-infrared and radio properties of the optically selected quasars at z∼6, focusing on luminosity correlations and evolution. We will also discuss the radio loud fraction of quasars. We will present further analysis of the FIR to radio SEDs and discuss possible star forming activity in a second paper (paper II). The sample and observations are described in section 2, and results are presented in section 3. In section 4 and 5, we analyse and discuss the general properties of FIR and radio luminosities for the entire sample and give the conclusion in section 6. We adopt a concordance cosmology with $H_0 = 71\,\mathrm{km\,s^{-1}\,Mpc^{-1}}$, $\Omega_m = 0.27$ and $\Omega_\lambda = 0.73$ throughout this paper.

2. Sample and Observation

The sample of z∼6 quasars are selected from about 6600 deg^2 of imaging data from the Sloan Digital Sky Survey (Fan et al. 2006b). Fan et al. (2000, 2001, 2003, 2004, 2006a) selected sources with very red $i - z\,colors$ as z≥ 5.7 quasar candidates. These candidate sources were followed up with high quality spectroscopy. Nineteen z∼6 quasars have been published by the SDSS survey (Fan et al. 2000, 2001, 2003, 2004, 2006a) with redshifts ranging from 5.74 to 6.42 and rest frame B band optical luminosities[1] from $10^{12.5}\,\mathrm{L_\odot}$ to $10^{13.3}\,\mathrm{L_\odot}$. Most of the 13 objects we observed in this work were discovered in the past two years (Fan et al. 2004; 2006a) and have not been observed in the (sub)mm or radio bands before.

We compare the (sub)mm properties of the z∼6 objects with luminous ($L_B \geq 10^{12.5}\,\mathrm{L_\odot}$) quasars at lower redshifts from the literature. We define a low redshift group, $1.5 \leq \mathrm{z} \leq 3.0$, using a sample from Omont et al. (2003) containing radio-quiet quasars with B-band absolute magnitude $-29.5 \leq \mathrm{M_B} \leq -27.0$ and redshift $1.8 \leq \mathrm{z} \leq 2.8$ observed by MAMBO at 250GHz, and a sample from Priddey et al. (2003a) of radio-quiet quasars with $-29.2 \leq$

[1] $\mathrm{L_B} \equiv \nu \mathrm{L}_{\nu,4400\mathrm{\AA}}$: $L_{\nu,4400\mathring{A}}$ is the luminosity density at rest frame 4400Å. we calculate $L_{\nu,4400\mathring{A}}$ and L_B from the AB magnitude at rest frame $1450\mathring{A}$ in the discovering papers (Fan et al. 2000, 2001, 2003, 2004, 2006a), assuming an optical spectral index of -0.5.

$M_B \leq -27.5$ and $1.5 \leq z \leq 3.0$. Our higher redshift group ($3.6 \leq z \leq 5.0$) is drawn from the the Palomar Sky Survey (PSS) selected sample of Omont et al. (2001) ($M_B \leq -27.0$; $3.9 \leq z \leq 4.6$) and the SDSS sample of Carilli et al. (2001) ($-28.8 \leq M_B \leq -26.1$; $3.6 \leq z \leq 5.0$), both observed with MAMBO at 250 GHz. The 3σ detection limits of the MAMBO observations by Omont et al. (2001) and (2003) are ∼1.5 to 4 mJy, and ∼1.4 mJy by Carilli et al. (2001). The typical 3σ detection limit of SCUBA observations reported by Priddey et al. (2003a) is ∼ 10 mJy at 350 GHz, which corresponds to an upper limit of ∼4 mJy at 250 GHz (assuming a warm dust SED with temperature $T_d = 47$K and emissivity index $\beta = 1.6$).

A total of 13 z∼6 SDSS quasars were observed in the course of the work presented here, all with the VLA at 1.4GHz and eleven (all but J000552.34-000655.8 and J104845.05+463718.3) with MAMBO-2 at 250GHz (See Table 1 for the source list). J104845.05+463718.3 was a published detection by MAMBO (Bertoldi et al. 2003a) and was observed by the VLA with a signal at 2.2σ (Carilli et al. 2004). We re-observed it with the VLA, and combined all the data.

MAMBO-2 at the IRAM 30m telescope is a 117-channel bolometer array. The Half Power Beamwidth (HPBW) of each pixel is $11''$ and the spacing between horns is about $20''$. The effective sensitivity is about 40 $\mathrm{mJys}^{1/2}$. The new observations were made in the winters of 2004-2005 and 2005-2006 during pooled observations using the on-off mode, wobbling by $32'' - 46''$ in azimuth and at a rate of 2 Hz. The target sources are positioned on the most sensitive bolometer and the correlated sky noise is determined from the other bolometers and subtracted from the source bolometer. The median rms is ∼0.8 mJy (Table 1). We reduced the data with the MOPSIC software package (Zylka 1998) and standard scripts for on-off observation data.

The VLA observations were made with the A array, of which the maximum baseline is 30 km. The sources were observed at 1.4 GHz with two Intermediate Frequency bands "IFs" and 50MHz bandwidth per IF. The corresponding Full Width at Half Maximum (FWHM) resolution is about $1.4''$. We observed each source for two to four hours to a typical rms noise level of ∼16 $\mu\mathrm{Jy\,beam}^{-1}$ (Table 1). The data were reduced and images were made using the standard VLA wide field data reduction software AIPS.

3. Results

We present our MAMBO-2 results of 11 sources and the VLA results of 13 sources in Table 1. The optical properties are taken from Fan et al. (2006b) and presented in Col. (1):

the SDSS name, Col. (2): the redshift, and Col. (3): the AB magnitude at 1450Å. Col. (4) lists the radio 1.4GHz surface brightness at the optical position. Col. (5), (6), and (7) list the nearest radio peak position and peak surface brightness for detected sources. Col. (8) presents the 250GHz flux densities in mJy. We mark detections in bold face. For the source J000552.34-000655.8, there is a strong (∼Jy) radio source in the field which precludes deep VLA radio imaging. The rms on the 1.4GHz map is 130 μJy, which is an order of magnitude higher than the others, yielding an extremely high upper limit of ∼390 μJy. Thus, we exclude this source in all of our analyses in this paper.

We show the radio 1.4GHz continuum images of the 12 remaining sources in Figure 1. We searched for $\geq 3\sigma$ peaks within a $0''.6$ radius from the optical quasar position in the radio map. This is a combination of the positional uncertainty of $0''.3$ between the radio and optical reference frames (Deutsch 1999) and the radio observation uncertainty of $\sigma_{\rm pos} \sim \frac{\rm FWHM}{\rm SNR} \sim 0''.5$[2]. Six sources are detected at the $\geq 3\sigma$ level. According to the 1.4 GHz radio source counts (Fomalont et al. 2006, in prep.), we expect 0.003 detections with $\rm S_{1.4GHz} \geq 50\,\mu Jy$ by chance, within the total search area around the 12 quasars.

We obtain four detections among the 11 sources with MAMBO. Three of the detections, J084035.09+562419.9 J092721.82+200123.7 and J133550.81+353315.8, are detected at $> 4\sigma$. The fourth source, J081827.40+172251.8, is marginally detected at the $\sim 3\sigma$ level. As a comparison, the cumulative number counts of 250 GHz source is about 400 $\rm deg^{-2}$ with flux density $\rm S_{250GHz} \geq 2.4\,mJy$ (Greve et al. 2004; Voss et al. 2006) which is the typical 3σ limit of our observations. Thus we should expect 0.03 detections in our 11 fields by chance, given the $11''$ beam size of the MAMBO bolometer elements.

We summarize the (sub)mm and radio observations of the six previously observed quasars in the z∼6 SDSS sample (Petric et al. 2003; Priddey et al. 2003b; Bertoldi et al. 2003a; Robson et al. 2004; Carilli et al. 2004) in Table 2. Col. (1), (2), and (3) give the name, redshift, and 1450Å AB magnitude, and Col. (4), (5), (6), and (7) the flux densities at 250 GHz, 350 GHz, 667 GHz and 1.4 GHz.

Combining Tables 1 and 2, there are seventeen z∼6 quasars that have been observed with MAMBO. Together with the results from SCUBA at 850 μm, there are eighteen z∼6 SDSS quasars that have (sub)mm observations at the 1 mJy sensitivity level and 8 of them are detected at $\gtrsim 3\sigma$. The detection rate is $44 \pm 16\%$. The detection rate of optically bright quasar samples at redshifts 2 and 4 is $\sim 30\%$ in Omont et al. (2001, 2003) with an rms level of $> 1.5\,mJy$, and $\sim 39\%$ in Carilli et al. (2001) with a lower rms level of $\sim 1.4\,mJy$. Thus our detection rate at z∼6 is slightly higher compared to these observations at lower

[2]We require a signal to noise ratio (SNR) of 3 for detections here.

redshifts, but is consistent within the errors.

Seventeen sources in the z∼6 SDSS quasar sample have deep observations with the VLA at 1.4 GHz and 8 are detected at the $\gtrsim 3\sigma$ level. J083643.85+005453.3 is the only >1 mJy radio source at 1.4 GHz among them. It was detected by Petric et al. (2003), as well as in the FIRST survey (White et al. 1997), leading to a weighted average flux density of 1.74±0.04 mJy[3]. Another source, J163033.90+401209.6, has not been observed with the VLA yet, and the FIRST catalog yields an upper limit of 0.44 mJy at the optical position (Bertoldi et al. 2003). We thus exclude this source in the analysis of radio properties in the next section.

4. Analysis

4.1. The FIR emission

To estimate the FIR luminosity of our z∼6 quasars, we model the FIR continuum with an optically thin grey body (Eq. (1)), adopting a dust temperature of $T_d = 47$K and emissivity index, $\beta = 1.6$, which is derived from the mean SED of high-redshift quasars (Beelen et al. 2006). We normalize the SED to the (sub)mm data and integrate the model SED from rest frame 42.5 μm to 122.5 μm to get the total FIR flux[4]:

$$\mathrm{FIR} \propto \int \nu^{3+\beta} \frac{1}{\exp(h\nu/kT_d) - 1} d\nu \quad (1)$$

This estimation of FIR emission is sensitive to the assumed dust temperature (T_d). A higher temperature, eg. $T_d = 55$K, will increase the estimated FIR flux by a factor of ∼1.5. For non-detections ($< 3\sigma$), we adopt as upper limits the larger value of either (a) the 2σ rms or (b) the measured value at the optical position plus 1σ rms for all the following calculations and plots. The FIR luminosities (L_{FIR}) are given in table 4; most of the (sub)mm detected sources are very luminous in the FIR band, with implied $L_{FIR} \sim 10^{13}\, L_\odot$ (see Table 4). We estimated the FIR luminosities for all the low redshift comparison samples in the same way.

We plot the FIR luminosity (L_{FIR}) versus redshift in Figure 2, including the z∼6 SDSS sample and all the comparison samples. In Figure 3, we present the histograms of the L_{FIR} and L_{FIR}/L_B distributions separately for different redshift intervals. For the (sub)mm

[3]The 1.4 GHz flux density for J083643.85+005453.3 is $1750 \pm 40\,\mu$Jy in Petric et al. (2003) and $1530 \pm 150\,\mu$Jy in the FIRST catalog.

[4]For J114816.64+525150.3, we directly adopt the fitting results from Beelen et al. (2006) with $T_d = 55$K and $\beta = 1.6$.

detections at all redshifts, the L_{FIR} values lie between $10^{12.5}\,L_\odot$ and $10^{13.8}\,L_\odot$. The $1.5 \leq z \leq 3$ group covers an even narrower range with most of the detected sources distributed at $L_{FIR} \geq 10^{13}\,L_\odot$ These ranges are partially a result of the detection thresholds, i.e. a detection limit of 1.5mJy at 250GHz corresponds to FIR luminosities $\sim 10^{12.5}\,L_\odot$ for redshifts from 4 to 6 and $\sim 10^{13}\,L_\odot$ at z∼2. However, the L_{FIR}/L_B distributions are similar for the (sub)mm detections at all redshifts (See Fig. 3 (b)). A similar conclusion was obtained by Omont et al. (2003) and Beelen et al. (2004), but we are extending it to the quasar sample at z∼6. This fact suggests the optical to FIR spectra energy distributions (SEDs) of the luminous quasars in both optical and FIR bands do not evolve much from z∼2 to 6.

L_{FIR} versus L_B is plotted in Figure 4, for quasars at all redshifts. We present correlation tests for (i) the z∼6 sample only (z∼6), (ii) samples at all redshifts (Total), and (iii) (sub)mm detections in all samples (Detection). We apply the General Kendall's tau test (Isobe et al. 1986), taking L_B as the independent variable and L_{FIR} as the dependent variable. The results are listed in Table 3 with Col. (1) the sample used, Col. (2) the sample size, and Col. (3) the Kendall's tau value. The probabilities (P_{null}) that no correlation exists between L_B and L_{FIR} (the null hypothesis) are given in Col. (4). We take $P_{null} = 5\%$ as the significance level below which the null hypothesis can be rejected.

There is no correlation between L_B and L_{FIR} for the z∼6 sample only ($P_{null} \sim 44\%$). However, the P_{null} value is 6% when all the samples are included, which suggests a marginal correlation. These results indicates that the FIR and optical emission of these (sub)mm observed quasars are correlated, but the scatter is large enough that the correlation is not seen over a narrow luminosity range. This correlation is even more significant when we do the test with only the (sub)mm detections at all redshifts ($P_{null} \sim 0.02\%$). But one should be careful with this result as there may be a number of observational or selection bialses in the sample of detections. For example, given the similar observational sensitivity level, the FIR luminosity threshold for the (sub)mm detections is decreasing with redshifts at $z > 2$ (see Figure 1). We apply linear regression to all of the (sub)mm observed samples (Total) and the subsample of detections (Detection), using the Expectation-Maximization (EM) method which can deal with data including upper limits (Isobe et al. 1986). The best fitting results are:

$$\text{Total}: \ \log\left(\frac{L_{FIR}}{L_\odot}\right) = (0.21 \pm 0.15)\log\left(\frac{L_B}{L_\odot}\right) + (9.67 \pm 2.03) \quad (2)$$

$$\text{Detection}: \ \log\left(\frac{L_{FIR}}{L_\odot}\right) = (0.40 \pm 0.09)\log\left(\frac{L_B}{L_\odot}\right) + (7.82 \pm 1.20) \quad (3)$$

The regression results show a non-linear relationship between the FIR emission and the quasars' optical emission with slopes much smaller than unity. We plot the fitting results

in Figure 4. As a comparison, We calculate the typical FIR-to-B band luminosity ratios for local optical quasars based on the radio quiet and radio loud quasar templates in Elvis et al. (1994). The FIR luminosities are integrated directly from the template SEDs. The derived FIR-to-B band luminosity ratios (L_{FIR}/L_B) are 0.29 and 0.38 for the radio quiet and radio loud templates respectively, and are ploted as $L_{FIR} = 0.29L_B$ (solid line) and $L_{FIR} = 0.38L_B$ (long dashed line) in Figure 4. According to Figure 4, most of the (sub)mm detections have larger L_{FIR}/L_B value than that of the local optical quasar templates. For the eight (sub)mm detected quasars at z∼6, six of them have FIR emission stronger than that predicted from the radio quiet template (by factors from ~ 1.5 to $\gtrsim 5$), and only one source J081827.40+172251.8 is consistent with the template within errors.

4.2. The Radio emission

The rest frame 1.4GHz luminosities (L_{Rad}[5]) for the 17 quasars observed with the VLA in the z∼6 sample are calculated, assuming a power law ($f_\nu \sim \nu^\alpha$) radio SED and a radio spectral index of $\alpha = -0.75$ (Condon 1992). Since all the sources are unresolved on the radio maps (Figure 2), we adopt the peak surface brightness in Table 1 as the 1.4GHz flux density for our VLA detections and take the larger value of either the 2σ rms on the radio map or the measured value at the optical position plus 1σ rms as the upper limits for non-detections. The rest frame radio to B band optical luminosity density ratios $R^*_{1.4} = L_{\nu,1.4GHz}/L_{\nu,4400\mathring{A}}$ (Cirasuolo et al. 2003; 2006) are calculated and listed in Table 4. $L_{\nu,4400\mathring{A}}$ is the luminosity density at rest frame 4400Å (See the footnote in Section 2). We adopt $R = L_{\nu,5GHz}/L_{\nu,4400\mathring{A}} = 10$ (Kellermann et al. 1989) to separate radio loud and radio quiet sources. This corresponds to $R^*_{1.4} \sim 30$ by assuming the above radio spectral index and converting the rest frame 5 GHz flux density to 1.4 GHz.

We plot the rest frame 1.4 GHz radio luminosity (L_{Rad}) vs. B band luminosity (L_B) in Figure 5. The typical 3σ detection limit of the VLA observation is $\sim 50\,\mu$Jy (dotted line), which is roughly 10 times deeper than the FIRST survey (solid line). Thus our VLA observations are sensitive enough to detect any radio loud source with B band luminosity $> 10^{12}\,L_\odot$ at z∼6 for all of the 17 sources. We plot the $R^*_{1.4}$ distribution of the 17 z∼6 quasars in Figure 6. None of the 13 sources with new radio data reported in this paper is radio-loud. For the whole sample of 17 z∼6 quasars, there is one marginally radio-loud object, J083643.85+005453.3, with $R^*_{1.4} \sim 40$.

[5] $L_{Rad} \equiv \nu L_{\nu,1.4GHz}$ in rest frame

The deep VLA observations also enable us to investigate the correlation between radio and FIR emission of the z∼6 quasars. Yun et al. (2001) employ a q parameter to quantify the ratio of the FIR and radio luminosities:

$$\mathrm{q} \equiv \log(\frac{\mathrm{FIR}}{3.75 \times 10^{12}\,\mathrm{W\,m^{-2}}}) - \log(\frac{\mathrm{f_{1.4GHz}}}{\mathrm{W\,m^{-2}\,Hz^{-1}}}). \quad (4)$$

Yun et al. (2001) studied the infrared-selected galaxies in the IRAS 2Jy sample and found a q value of 2.34 for typical star forming galaxies. We calculate the q values for the 12 z∼6 quasars that are detected at either radio or (sub)mm wavelengths.

We also plot $\mathrm{L_{FIR}}$ vs. the rest frame 1.4GHz radio luminosity density ($\mathrm{L_{\nu,1.4GHz}}$) in Figure 6, comparing the z∼6 quasar sample to typical star forming galaxies in the local universe (Yun et al. 2001). The solid line in Figure 6 corresponds to the typical q value of 2.34 in star forming galaxies, and the dotted lines denote excesses that are 5 times above and below this typical correlation (Yun et al. 2001).

There are four sources in the z∼6 quasar sample that are detected in both the radio and (sub)mm regimes. One of them, J081827.40+172251.8, has a small q value that falling beyond the range defined by typical star forming galaxies, indicating the dominance of AGN power in the FIR to radio SED of this source. However, the FIR-to-radio ratios of the other three sources, though slightly above the mean value of q = 2.34, are consistent with star forming galaxies (Figure 6 and Table 4).

5. Discussion

The heating sources of the FIR emitting dust in quasars are studied and the contributions from host galaxy star formation are discussed in a number of papers (eg. Haas et al. 2003; Omont et al. 2003; Schweitzer et al. 2006). Star formation is believed to be the dominated dust heating resource in the local infrared luminous quasars that are located in ULIRGs (Hao et al. 2005). Schweitzer et al. (2006) studied the connection between FIR emission and PAH/low excitation fine-structure emission lines of the local PG quasars. Their results suggest that star formation is responsible for at least 30% to the average local quasar FIR emission and that this contribution tends to increase with FIR luminosity. The z∼6 SDSS quasars we discussed in this paper belong to the population of the brightest quasars in the optical. About 1/3 of them are detected at (sub)mm wavelength. According to Figure 4, most of these detections have FIR luminosities stronger than the predictions from local quasar templates, indicating extra emission from warm dust in these sources compared to the typical optical quasar emission. Moreover, the relationship between the FIR

and B band optical emission is non-linear and significantly scattered, only manifesting itself when a larger luminosity range is considered (See Section 4.1). Beelen (2004) studied a number of optically bright quasar samples at z > 1.5 that had (sub)mm observations, and first report this weak correlation between FIR and B band optical emission, namely $\log L_{FIR} = (8.36 \pm 0.90) + (0.33 \pm 0.07) \times \log L_B$ (See also Cox et al. 2005). The results are consistent when we include our new observations at z∼6. Additionally, most of the (sub)mm detections at z∼6 have FIR-to-radio ratios or upper limits within the range occupied by star forming galaxies (See Table 4 and Figure 6).

One possible explanation for all of these facts is that star formation is happening on a massive scale in the host galaxies of these FIR luminous z∼6 quasars and dominating the heating process of the FIR emitting warm dust. The implied star formation rate is $\sim 10^3\,M_\odot\,yr^{-1}$. This idea is supported by the detections of CO in the high-redshift quasars that have strong FIR emission ($L_{FIR} \gtrsim 10^{13}\,L_\odot$). CO line emission was detected in several FIR luminous quasars at z$\gtrsim$4, including the highest redshift quasar J114816.64+525150.2 (eg. Riechers et al. 2006; Bertoldi et al. 2003b; Walter et al. 2003, 2004). The CO detections indicate huge amount of molecular gas in the host galaxies of these FIR luminous quasars which are the requisite fuel for star formation. Moreover, Riechers et al. (2006) found that the FIR-to-CO relation of the high-redshift FIR luminous quasars are consistent with that defined by ULIRGs, starforming galaxies and submillimeter galaxies.

One may argue that the strong FIR emission can be also processed by the AGN power since the dust torus geometry of these sources are still unkown. This possibility cannot be rule out given the limited data we have for these sources, but detailed dust models are required to explain the results we list above. One fact is that the hot dust emission of the SDSS z∼6 quasars probed by recent Spitzer observation are similar to those of the local quasar templates as we mentioned in Section 1 (Jiang et al. 2006a). Four (sub)mm detections are included in this Spitzer observed sample, and no different properties are found in the optical to near infrared SEDs of these sources. This may not support the idea of a quite different geometry of the dust torus.

However, we should mention that there are still large uncertainties in the estimations of the FIR luminosities for these (sub)mm detected z∼6 quasars. The FIR luminosities for some of the sources can be overestimated given the poor data at (sub)mm wavelengths. Thus further studies on these (sub)mm detected z∼6 quasars are required, including observations of the submm continuum at higher frequencies and emission lines of CO and other molecules, such as HCN, as well as the C and C^+ fine structure lines.

Another interesting question is how the current radio observations constrain the radio loud fraction (RLF) at z∼6. The RLF of optically selected quasar samples is $\sim$ 10%, as

quoted in many papers (Kellermann et al. 1989; Ivezić et al. 2002, 2004; Cirasuolo et al. 2003, 2006). Jiang et al. (2006b) studied the FIRST data (Becker et al. 1995) for SDSS quasars with redshifts up to 5, and suggested that the quasar RLF increases with optical luminosity and decreases with redshift, namely $\log((\mathrm{RLF})/(1-\mathrm{RLF})) = (-0.112\pm0.109)+(-2.196\pm0.269)\log(1+\mathrm{z})+(-0.203\pm0.026)(\mathrm{M}_{2500}+26)$. This result gives an RLF of $\sim 37\%$ at z = 0.5, $\sim 11\%$ at z = 2, and $\sim 2\%$ at z = 6, given the rest frame 2500Å absolute AB magnitude $\mathrm{M}_{2500} = -27.3$ — the typical value of the z∼6 SDSS quasar sample[6].

There is one marginally radio loud source in this z∼6 sample of 17 sources. This result argues against a high RLF, i.e. $> 20\%$, for the current SDSS quasar sample at z∼6. Thus it is roughly consistent with the result of Jiang et al. (2006b). However, the sample size is still too small to set a strict constrain, i.e. differentiate an RLF between $\sim 2\%$ and $\sim 10\%$. Thus to provide a better test of the redshift evolution of the RLF; we would need a sample three times larger to usefully constrain the RLF at z∼6.

We should also mention the recent discovery of a radio loud quasar at z>6, FIRST J1427385+331241(McGreer et al. 2006), with a FIRST flux density of 1.73mJy. This source is the most radio luminous quasar known at z∼6, with $\mathrm{R}^{*}_{1.4} > 100$. However, it cannot be included in our radio loud analysis at z∼6, as the selection criteria of this source are quite different from that of the SDSS quasars and its UV/Optical emission is just beyond the SDSS detection limits (McGreer et al. 2006).

6. Conclusion

In this paper, we present new results of millimeter and radio observations of a sample of z∼6 quasars. These quasars are selected from the SDSS survey and observed with MAMBO-2 at 250 GHz and the VLA at 1.4 GHz. We obtained three $> 4\sigma$ detections and one $\sim 3\sigma$ detection out of 11 observed sources by MAMBO-2 and six radio detections out of 13 observed sources by the VLA.

We combine our new millimeter and radio results of the SDSS z∼6 quasars with results from the literature and discuss the FIR and radio properties of the optically selected quasars at z∼6. Our conclusions are as follows.

- Eight out of 18 z∼6 optically selected quasars are detected in the (sub)mm regime. This indicates a (sub)mm detection rate of 44% at z∼6 at mJy sensitivity. Within

[6]The M_{2500} is estimated from the absolute AB magnitude at rest frame 1450Å (M_{1450}, Fan et al. 2006b). For the current sample of 19 z∼6 SDSS quasars with M_{1450} from -26.2 to -27.9, we adopt a typical value of $\mathrm{M}_{1450} = -27.0$ and an optical spectral power law index of -0.5.

the errors, this is consistent with the ∼30% (sub)mm detection rate at lower reshift (eg. Carilli et al. 2001; Omont et al. 2001; 2003). The observational data imply FIR luminosities $\sim 10^{13}\,L_\odot$ in the (sub)mm detected sources.

- We compare the distribution of FIR luminosities and FIR to optical ratios between the z∼6 SDSS sample and (sub)mm observed optically bright quasars ($L_B \geq 10^{12.5}\,L_\odot$) at lower reshifts. The distributions of the FIR-optical ratio are similar for different redshift groups, which suggests that the average optical-to-FIR SED of optically bright quasars is independent of redshift.
- We extend the quasar FIR-to-optical correlation study to the z∼6 SDSS sample. No correlation is found with the z∼6 sample only. However, a correlation (albeit with large scatter) can be seen when all the samples extending from z=1.5 to 6.42 are included.
- We also discussed the FIR-to-radio ratios of the z∼6 quasars, by comparing them to the typical correlation defined by star forming galaxies. Three of the four sources that are detected in both the millimeter and radio bands have FIR-to-radio ratios within the range defined by star forming galaxies.
- We found no strong radio sources with $R^*_{1.4} \geq 30$ among the new SDSS sources of bright z∼6 quasars. In the whole z∼6 sample, only one radio detection has a radio to optical ratio $R^*_{1.4} \sim 40$ and no source has $R^*_{1.4} \gtrsim 100$. These data are consistent with, although do not set strong constraints on, the recent conclusion of a decreasing radio loud quasar fraction with increasing redshift (Jiang et al. 2006b).

These results give a view of the general FIR through radio properties of the z∼6 SDSS quasars. The data are consistent with the idea that massive starbursts may exist in the host galaxies of the strong (sub)mm detections at z∼6 and contribute to the FIR and radio emission. These strong (sub)mm sources provide the only candidates to search for CO and C^+ into the epoch of reionization, and to test the idea of co-eval SMBH and host galaxy formation. We may expect to go an order of magnitude deeper in a few years time with the coming instruments of the Expanded Very Large Array (EVLA) and the Atacama Large Millimeter Array (ALMA).

We acknowledge support from the Max-Planck Society and the Alexander von Humboldt Foundation through the Max-Planck-Forschungspreis 2005. The National Radio Astronomy Observatory is a facility of the National Science Foundation, operated by Associated Universities, Inc. We thank Dr. R. Zylka at IRAM for his help with the MAMBO data reduction. Ran Wang thanks her supervisor, Prof. Xue-Bing Wu and the whole AGN group at Peking University for helpful discussions. X. Fan acknowledge support from NSF grant AST 03-07384, a Sloan Research Fellowship, and a Packard Fellowship for Science and Engineering.

Facilities: VLA, IRAM (MAMBO), SDSS.

REFERENCES

Beelen, A. 2004, PhD thesis, Observatoire de Paris

Beelen, A., Cox, P., Benford, D. J., Dowell, C. D., Kovács, A., Bertoldi, F., Omont, A., & Carilli, C. L. 2006, ApJ, 642, 694

Bechtold, J. et al. 2003, ApJ, 588, 119

Becker, R. H., White, R. L., & Helfand, D. J. 1995, ApJ, 450, 559

Bertoldi, F., Carilli, C. L., Cox, P., Fan, X., Strauss, M. A., Beelen, A., Omont, A., & Zylka, R. 2003a, A& A, 406, L55

Bertoldi, F. et al. 2003b, A& A, 409, L47

Blain, A. W., & Longair, M. S. 1993, MNRAS, 264, 509

Blain, A. W., Smail, I., Ivison, R. J. et al. 2002, Phys. Rept. 369, 111

Carilli, C. L. et al. 2001, ApJ, 555, 625

Carilli, C. L. et al. 2004, AJ, 128, 997

Cirasuolo, M., Celotti, A., & Magliocchetti, M. 2003, MNRAS, 346, 447

Cirasuolo, M., Magliocchetti, M., Gentile, G., Celotti, A., Cristiani, S., & Danese, L. 2006, MNRAS, 371, 695

Condon, J. J. 1992, ARA& A, 30, 575

Cox, P., Beelen, A., Bertoldi, F. 2005, The dusty and molecular Universe, ESA SP-577, 115

Deutsch, E. W. 1999, AJ, 118, 1882

Fan, X. et al. 2000, AJ, 120, 1167

Fan, X. et al. 2001, AJ, 122, 2833

Fan, X. et al. 2003, AJ, 125, 1649

Fan, X. et al. 2004, AJ, 128, 515

Fan, X. et al. 2006a, AJ, 131, 1203

Fan, X. et al. 2006b, AJ, 132, 117

Fan, X., Carilli, C. L., & Keating, B. 2006c, ARA& A, 44, 415

Ferrarese, L., & Merritt, D. 2000, ApJ, 539, L9

Fomalont, E. B. 2006, preprint

Gebhardt, K., Bender, R., Bower, G. 2000, ApJ, 539, 13

Greve, T. R., Ivison, R. J., Bertoldi, F., Stevens, J. A., Dunlop, J. S., Lutz, D., & Carilli, C. L. 2004, MNRAS, 354,779

Haas, M. et al. 2003, A& A, 402, 87

Hao, C. N., Xia, X. Y., Mao, Shude, Wu, Hong, Deng, Z. G. 2005, ApJ, 625, 78

Isaak, K. G., Priddey, R. S., McMahon, R. G., Omont, A., Peroux, C., Sharp, R. G., & Withington, S. 2002, MNRAS, 329, 149

Isobe, T., Feigelson, E. D., & Nelson, P. I. 1986, ApJ, 306, 490

Ivezić, Z. et al. 2002, AJ, 124, 2364

Ivezić, Z. et al. 2004, ASPC, 311, 347

Iwamuro, F,. Kimura, M., Eto, S., Maihara, T., Motohara, K., Yoshii, Y., & Doi, M. 2004, ApJ, 614, 69

Jiang, L. et al. 2006a, AJ, 132, 2127

Jiang, L., Fan, X., Ivezić, Z., Richards, G. T., Schneider, D. P., Strauss, M. A. & Kelly, B. C. 2006b, ApJ, 656, 680

Kellermann K. I., Sramek, R., Schmidt, M., Shaffer, D. B., & Green, R. 1989, AJ, 98,1195

Li, Y. et al. 2006, ApJ, submitted (astro-ph/0608190)

Magorrian, J. et al. 1998, AJ, 115, 2285

Maiolino, R. et al. 2005, A& A, 440, L51

Marconi, A., & Hunt, L. K. 2003, ApJ, 589, L21

McGreer, I. D., Becker, R. H., Helfand, D. J., & White, R.L. 2006, ApJ, 652, 157

Omont, A., Cox, P., Bertoldi, F., Cox, P., Carilli, C. L., Priddey, R. S., McMahon, R. C., & Isaak, K. G. 2001, A& A, 374, 371

Omont, A., Beelen, A., Bertoldi, F., McMahon, R. G., Carilli, C. L., & Isaak, K. G. 2003, A& A, 398, 657

Pentericci, L. et al. 2003, A& A, 410, 75

Petric, A. O., Carilli, C. L., Bertoldi, F., Fan, X., Cox, P., Strauss, M. A., Omont, A., & Schneider, D. P. 2003, AJ, 126, 15

Petric, A. O., Carilli, C. L., Bertoldi, F., Beelen, A., Cox, P., & Omont, A. 2006, AJ, 132, 1307

Priddey, R. S., Isaak, K. G., McMahon, R. G., & Omont, A. 2003a, MNRAS, 339, 1183

Priddey, R. S., Isaak, K. G., McMahon, R. G., Roboson, E. I., & Pearson, C. P. 2003b, MNRAS, 344, L74

Riechers, D. A. et al. 2006, ApJ, 650, 604

Robson, I., Priddey, R. S., Isaak, K. G., & McMahon, R. G. 2004, MNRAS, 351, L29

Schweitzer, M. et al. 2006, ApJ, 649, 79

Shemmer, O. et al. 2006, ApJ, 644, 86

Tremaine, S. et al. 2002, ApJ, 574, 740

Voss, H., Bertoldi, F., Carilli, C., Owen, F. N., Lutz, D., Holdaway, M., Ledlow, M., & Menten, K. M. 2006, A& A, 448, 823

Walter, F. et al. 2003, Nature, 424, 406

Walter, F., Carilli, C. L., Bertoldi, F., Menten, K., Cox, P., Lo, K. Y., Fan, X., & Strauss, M. A. 2004, ApJ, 615, L17

White, R. L., Becker, R. H., Helfand, D. J., & Gregg, M. D. 1997, ApJ, 475, 479

Willott, C. J., McLure, R. J. & Jarvis, M. J. 2003, ApJ, 587, L15

York, D. G. et al. 2000, AJ, 120, 1579

Yun, M. S., Reddy, N. A., & Condon, J. J. 2001, ApJ, 554, 803

Zylka, R. 1998, MOPSI Users Manual, (IRAM: Grenoble)

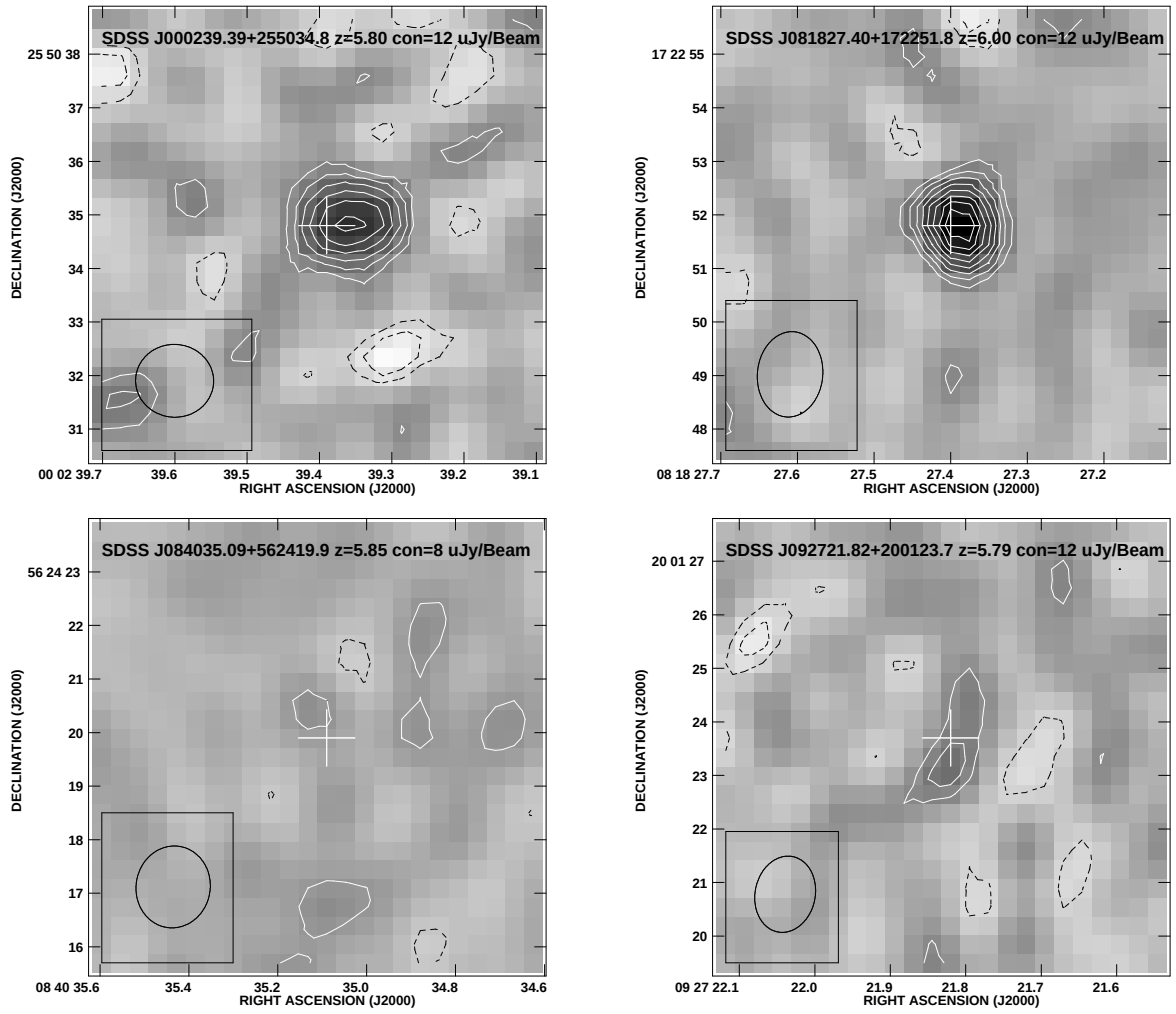

Fig. 1.— VLA images of 12 z∼6 quasars at 1.4GHz at 1.4″ resolution (FWHM). The parameter 'con' denotes the value for the contour increment in each map in units of μJy/Beam. The contour levels are (-3, -2, 2, 3, 4, 5, 6, 7, 8, 9, and 10) ×con. The ellipse indicates the beam in each case, and the cross marks the optical position.

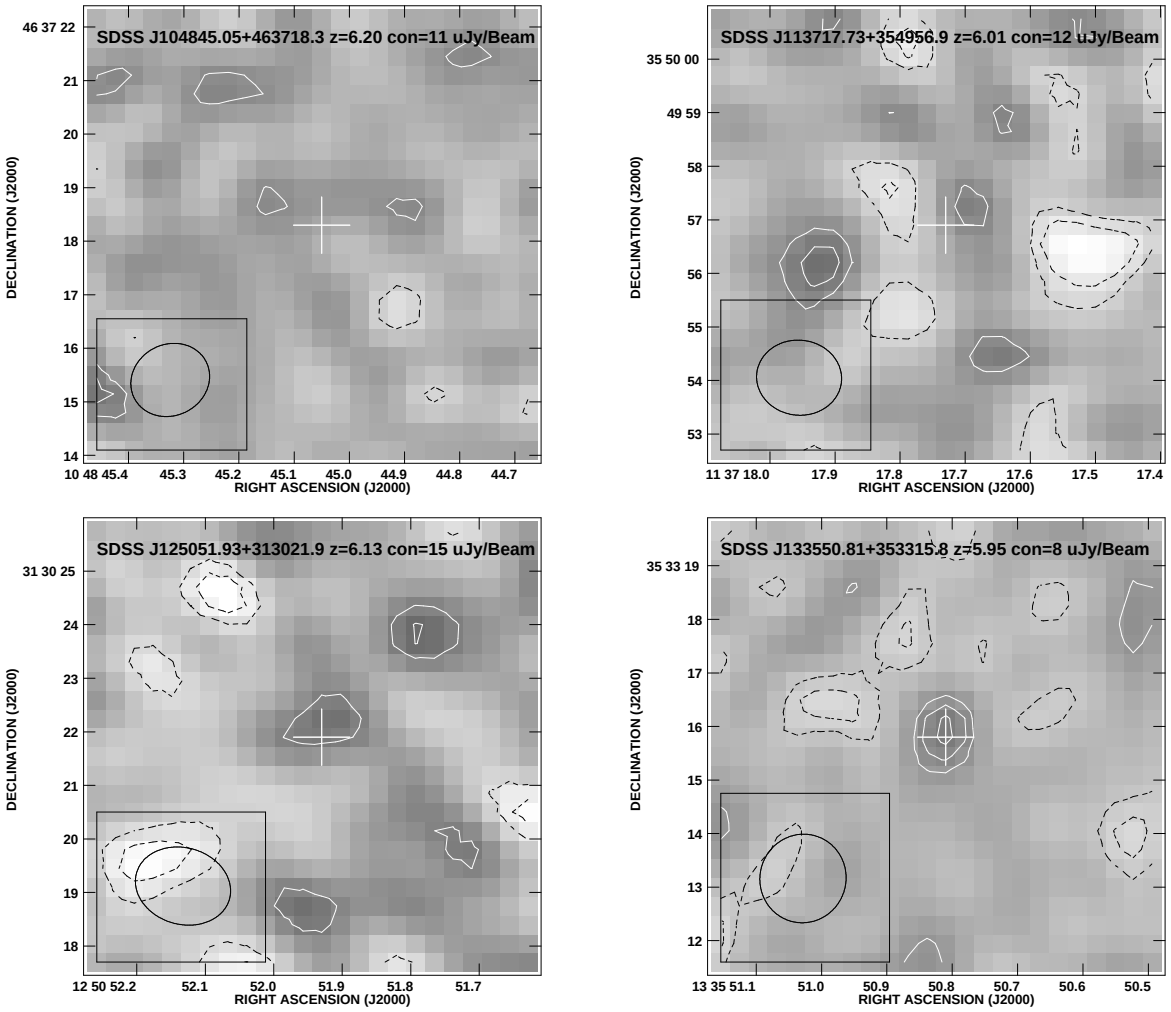

Fig. 1 – Continued

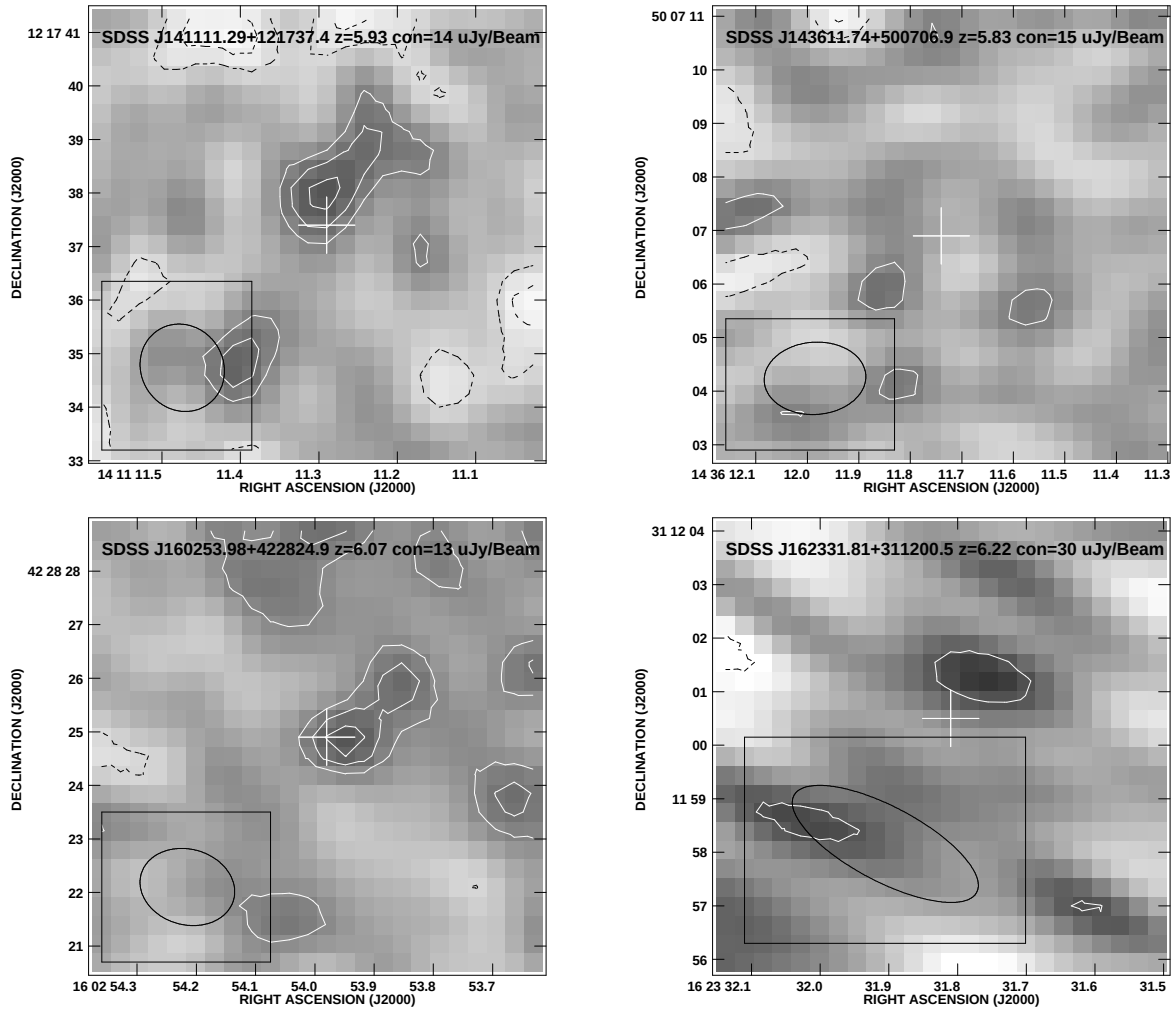

Fig. 1 – Continued

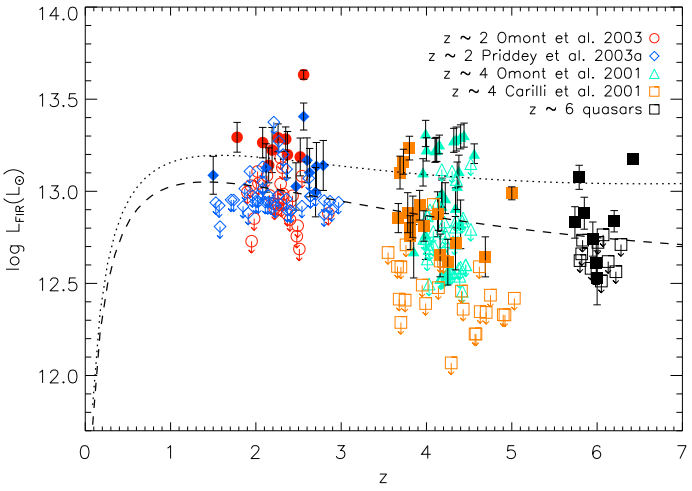

Fig. 2.— The logarithm of the FIR luminosity ($\log L_{\rm FIR}$) versus redshift for different samples. The filled symbols represent detections with 1σ errors. The open symbols with arrows denote upper limits: we adopt the larger value of either the 2σ rms or the measured value at the optical position plus 1σ rms as upper limits for non-detected sources. The dashed and dotted lines represent the typical 3σ detection limits of MAMBO at 250 GHz and SCUBA at 350 GHz, respectively, namely $S_{250\rm GHz} = 2.4\,$mJy (this work) and $S_{350\rm GHz} = 10\,$mJy (Priddey et al. 2003a).

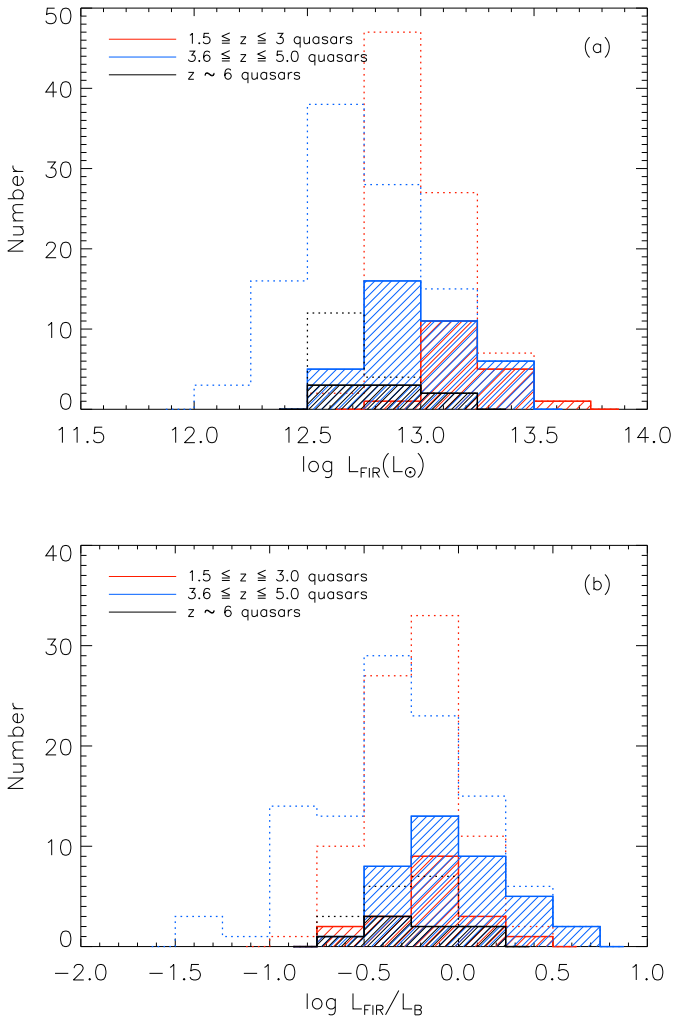

Fig. 3.— (a) The distribution of the logarithm of the FIR luminosity for quasars at different redshifts. The z∼6 quasars are plotted as black lines. The $1.5 \leq z \leq 3$ group (red lines) is combined with the samples from Omont et al. (2003) and Priddey et al. (2003a), while the $3.6 \leq z \leq 5$ group (blue lines) is from Omont et al. (2001) and Carilli et al. (2001). For all the samples, the shaded areas represent detections and dotted lines denote upper limits: the upper limits are calculated as in Figure 2. (b) The distribution of the logarithm of the FIR-optical ratio ($\log L_{FIR}/L_B$) for quasars at different redshifts.

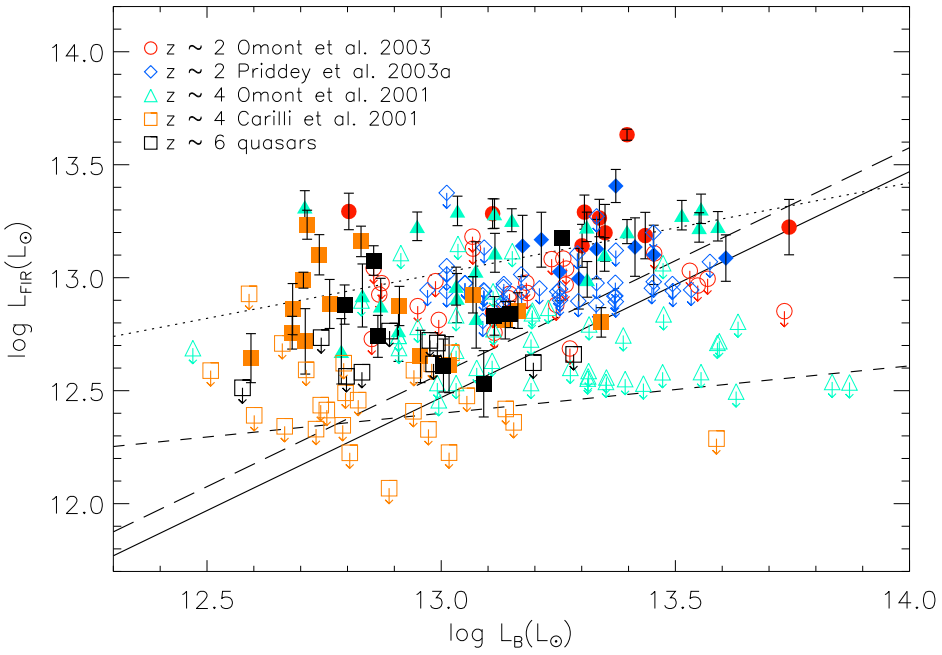

Fig. 4.— The logarithm of the FIR luminosity is plotted against the logarithm of the B band luminosity for all the (sub)mm observed quasars. The symbols are the same as in Figure 2. The dashed line is the linear regression result for the (sub)mm observed samples at all redshifts including upper limits, while the dotted line is the result using the detected objects only. The solid and long dashed lines represent the FIR-to-B band luminosity ratios of local radio quiet and radio loud quasar templates in Elvis et al. (1994), respectively.

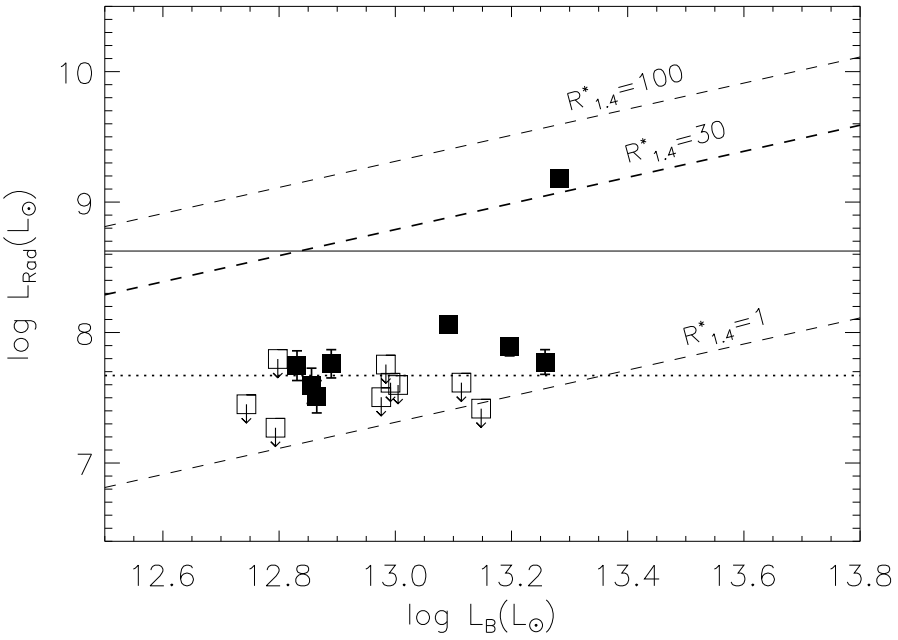

Fig. 5.— The logarithm of the rest frame 1.4GHz radio luminosity ($\log L_{\rm Rad}$) is plotted against the logarithm of the B band luminosity ($\log L_{\rm B}$) for the z$\sim$6 quasars observed with the VLA at 1.4GHz. The filled squares represent detections with 1σ errors, and the open squares with arrows denote upper limits: the upper limits are calculated as in Figure 2. The dashed lines represent rest frame radio-to-optical ratios ($R^*_{1.4}$) of 100, 30 (separation of radio loud and quiet), and 1. The dotted line denotes the typical 3σ detection limits of our VLA observations, while the solid line shows the 3σ detection limit of the FIRST survey.

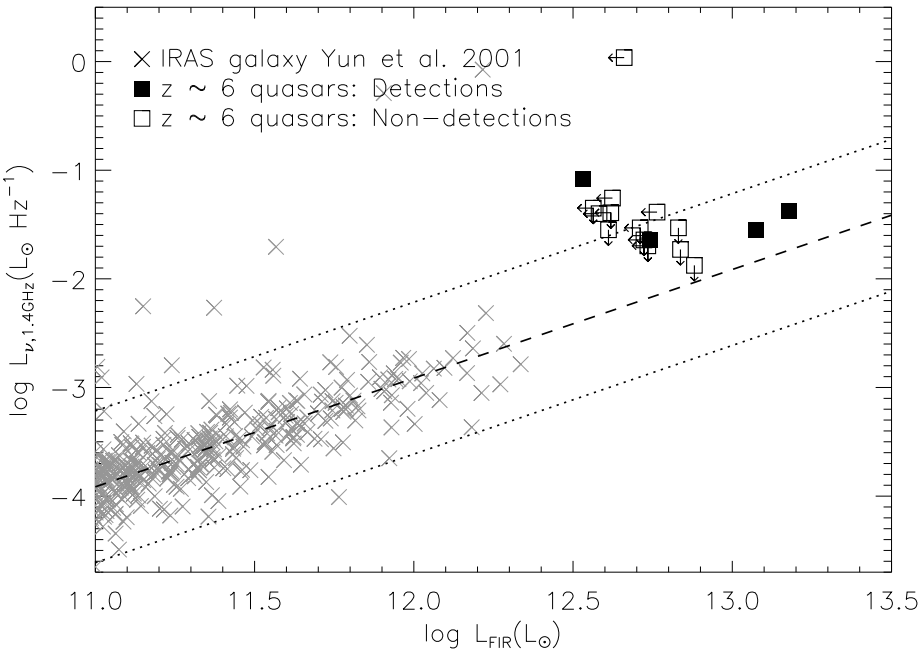

Fig. 6.— The logarithm of the rest frame 1.4 GHz radio luminosity density ($\log L_{\nu,1.4\mathrm{GHz}}$) versus the logarithm of the FIR luminosity ($\log L_{\mathrm{FIR}}$). The filled squares represent the detections in both radio and (sub)mm bands, and the open squares with arrows represent the upper limits of the non-detections in either radio or (sub)mm. The upper limits are calculated as in Figure 2. The crosses represent the IRAS 2Jy sample of galaxies in Yun et al. (2001) and the dashed line indicates the typical radio-to-FIR correlation in star forming galaxies, with correlation parameter q = 2.34 (Yun et al. 2001). The dotted lines represent excesses five times above and below the typical q value.

Table 1: 1.4GHz and 250GHz results of 13 z∼6 quasars.

SDSS name	z	$m_{1450Å}$	radio detection at 1.4 GHz				S_{250GHz}
			$S_{1.4opt}$ [b]	RA_{peak} [c]	Dec_{peak} [c]	S_{peak} [c]	
			μJy Beam^{-1}	h m s	° ′ ″	μJy Beam^{-1}	mJy
(1)	(2)	(3)	(4)	(5)	(6)	(7)	(8)
J000239.39+255034.8	5.80	19.02	81±14	00:02:39.36	25:50:34.9	**89**[d]	0.20±0.88
J000552.34−000655.8	5.85	20.03	40±130				
J081827.40+172251.8	6.00	19.34	119±12	08:18:27.39	17:22:51.8	**123**	**1.45±0.49**
J084035.09+562419.9	5.85	20.04	12±9				**3.20±0.64**
J092721.82+200123.7	5.79	19.87	33±14	09:27:21.82	20:01:23.1	**45**	**4.98±0.75**
J104845.05+463718.3	6.20	19.25	6±11				**3.00±0.40**[a]
J113717.73+354956.9	6.01	19.63	9±17				0.10±1.13
J125051.93+313021.9	6.13	19.64	37±21				0.07±0.90
J133550.81+353315.8	5.95	19.89	35±10	13:35:50.81	35:33:15.9	**35**	**2.34±0.50**
J141111.29+121737.4	5.93	19.97	44±16	14:11:11.29	12:17:38.0	**61**	1.00±0.62
J143611.74+500706.9	5.83	20.16	6±16				-0.21±1.14
J160253.98+422824.9	6.07	19.86	53±15	16:02:53.95	42:28:24.9	**60**	1.82±0.86
J162331.81+311200.5	6.22	20.13	24±31				0.17±0.80

[a]Result taken from Bertoldi et al. (2003a).

[b]Surface brightness at the optical quasar position plus the 1σ rms on the radio map.

[c]Position and surface brightness of the detected radio peak.

[d]The detections are marked as boldface.

Table 2: Published results from the literature.

SDSS name	z	$m_{1450Å}$	S_{250GHz}	S_{350GHz}	S_{667GHz}	$S_{1.4GHz}$
			mJy	mJy	mJy	uJy
(1)	(2)	(3)	(4)	(5)	(6)	(7)
J083643.85+005453.3	5.82	18.81	-0.4±1.0[a]	1.7±1.5[b]	-24±10[b]	**1740±40**[f,g]
J103027.10+052455.0	6.28	19.66	-1.1±1.1[a]	1.3±1.0[b]	-21±10[b]	-3±20[a]
J104433.04−012502.2	5.74	19.21	-	**6.1±1.2**[b]	-	-15±24[a]
J114816.64+525150.3	6.42	19.03	**5±0.6**[c]	**7.8±0.7**[d]	**24.7±7.4**[d]	**55±12**[e]
J130608.26+035626.3	5.99	19.55	-1.0±1.0[a]	**3.7±1.0**[b]	-7±14[b]	14±21[a]
J163033.90+401209.6	6.05	20.64	0.8±0.6[c]	2.7±1.9[d]	15.4±9.6[d]	< 440[c]

[a]Petric et al. (2003).

[b]Priddey et al. (2003b).

[c]Bertoldi et al. (2003a).

[d]Robson et al. (2004).

[e]Carilli et al. (2004).

[f]weighted average of the results in Petric et al. (2003) and the FIRST survey.

[g]The detections are marked as boldface.

Table 3: Correlation tests

Group (1)	Number (2)	Kendall's tau (3)	P_{null} (4)
z∼6	18	0.2222	0.4402
Total	208	0.1246	0.0575
Detection	64	0.6310	0.0002

Table 4: Derived parameters of the z∼6 quasars

SDSS name (1)	$\log L_B$ ($L_\odot$) (2)	$\log L_{FIR}$ ($L_\odot$) (3)	$\log L_{Rad}$ ($L_\odot$) (4)	$R^*_{1.4}$ (5)	q (6)
J000239.39+255034.8	13.20	<12.62	7.89	2.40	<1.31
J081827.40+172251.8	13.09	12.53	8.06	4.55	1.04
J083643.85+005453.3	13.28	<12.66	9.18	38.68	<0.05
J084035.09+562419.9	12.79	12.88	<7.27	<1.46	>2.18
J092721.82+200123.7	12.86	13.08	7.59	2.65	2.06
J103027.10+052455.0	12.99	<12.71	<7.62	<2.05	–
J104433.04-012502.2	13.11	12.83	<7.62	<1.55	>1.79
J104845.05+463718.3	13.15	12.84	<7.42	<0.90	>1.99
J113717.73+354956.9	12.98	<12.72	<7.50	<1.65	–
J114816.64+525150.2	13.26	13.18	7.77	1.60	1.98
J125051.93+313021.9	12.98	<12.62	<7.75	<2.87	–
J130608.26+035626.3	13.00	12.61	<7.60	<1.91	>1.59
J133550.81+353315.8	12.86	12.74	7.51	2.14	1.80
J141111.29+121737.4	12.83	<12.58	7.75	4.01	<1.41
J143611.74+500706.9	12.74	<12.73	<7.45	<2.48	–
J160253.98+422824.9	12.89	<12.76	7.76	3.62	<1.58
J162331.81+311200.5	12.80	<12.56	<7.80	<4.86	–
J163033.90+401209.6	12.58	<12.51	–	–	–

Note. — Col. (1), the name of the source, Col. (2), the B band luminosity (see the footnote in Section 2 for the calculation), Col. (3), the rest frame FIR luminosity, Col. (4), the rest frame 1.4 GHz radio luminosity, Col. (5), the radio-optical ratio $R^*_{1.4}$, and Col. (6) the FIR-to-radio correlation parameter q.